05

Towards the Development of an Active Terahertz RFTES Detector

© N.Yu. Rudenko,[1] S.V. Shitov[1,2]

[1] National University of Science and Technology MISiS,
119049 Moscow, Russia
[2] Kotelnikov Institute of Radio Engineering and Electronics, Russian Academy of Sciences,
125009 Moscow, Russia
e-mail: ny.rud@yandex.ru, sergey3e@gmail.com

Received September 17, 2024
Revised September 17, 2024
Accepted September 25, 2024

The model of the active superconducting terahertz detector comprising the RFTES (Radio Frequency Transition Edge Sensor) bolometer and the parametric microwave amplifier based on the DC-squid is analyzed. Electromagnetic modeling of the structure employing a quarter-wave resonator at a frequency of 1.5 GHz demonstrated the possibility of matching the losses introduced by the resistive bridge of the terahertz antenna and the resistive emulator of the squid. The numerical calculation of the DC-squid was performed using the RCSJ model accounting for nonlinear quasiparticle conductivity and a high-resistance shunt. The Josephson junctions are planned to be manufactured using the shadow sputtering technology $Al/AlO_x/Al$. The electrophysical parameters of the junction and the shunt, which are necessary for obtaining a hysteresis-free current-voltage characteristic of the DC-squid and implementing a gain of ~ 10 dB, have been estimated.

Keywords: DC-squid, RFTES bolometer, resonator, quasiparticle conductivity, Josephson junction, sandwich structure.

DOI: 10.61011/TP.2024.11.59747.275-24

Introduction

The receiving systems of future space missions using THz-band converters in the first stage should be equipped with a buffer amplifier with sensitivity near the quantum limit. The need to use a large number of low-frequency filters and room electronics is the main problem of the construction of TES (Transition Edge Sensor) matrices using DC-squids as preamplifiers, which significantly complicates the entire frequency multiplexing system, unlike the FDM reading technology implemented in MKID (Microwave Kinetic Induction Detector) type detectors and RFTES detectors [1], where semiconductor cooled microwave amplifiers are used. The next step may be to replace semiconductor amplifiers with fairly easy-to-configure parametric superconducting microwave amplifiers based on squids, which, as shown in [2,3], may have their own noise near the quantum limit. Microwave receivers use circuits in the standard $50\,\Omega$ in the vast majority of cases, which complicates matching the low active impedance of a single squid loop. This problem is overcome either by creating a traveling wave mode along an array of squids, or by including a single squid in a common resonant circuit with a signal source. The latter approach, using a single two-pin DC-squid as a preamp, seems more convenient for a frequency multiplexed matrix. Such a preamplifier can use a frequency multiplexer resonator and is naturally embedded in each pixel, which can provide quantum sensitivity of the entire matrix device.

It was proposed to combine two planar devices in [4]: a terahertz detector with microwave reading and a quantum parametric amplifier into a single device — an active superconducting detector (ASD) due to matching in a common resonator circuit. The versatility of this integration method allows for matching in a wide range of impedance of the sensing element and the amplifier connected to a single resonator.

1. Simulation of an active detector prototype

The design of the proposed active detector is shown in Fig. 1, *a*. A quarter-wave resonator based on a coplanar waveguide is inductively coupled to a transmission line. Near the open end, the resonator is loaded with a nanomode sensor embedded in a planar terahertz antenna, forming an RFTES detector [1]. It should be noted that the nanobridge is not galvanically coupled with an external system, which ensures its protection from low-frequency interference. A coupling element with a two-pin squid amplifier having a loop inductance of ~ 50 pH is placed near the shorted end at the other end of the resonator, near the current antinode. The location of the squid loop near the resonator current antinode makes it possible to capture small increments of the resonator magnetic field at the carrier frequency that occur when the bolometric sensor (nanobridge) is heated due to the terahertz current of the antenna. Thus, the high-quality resonator of the detector simultaneously performs both the function of frequency selection for the detector

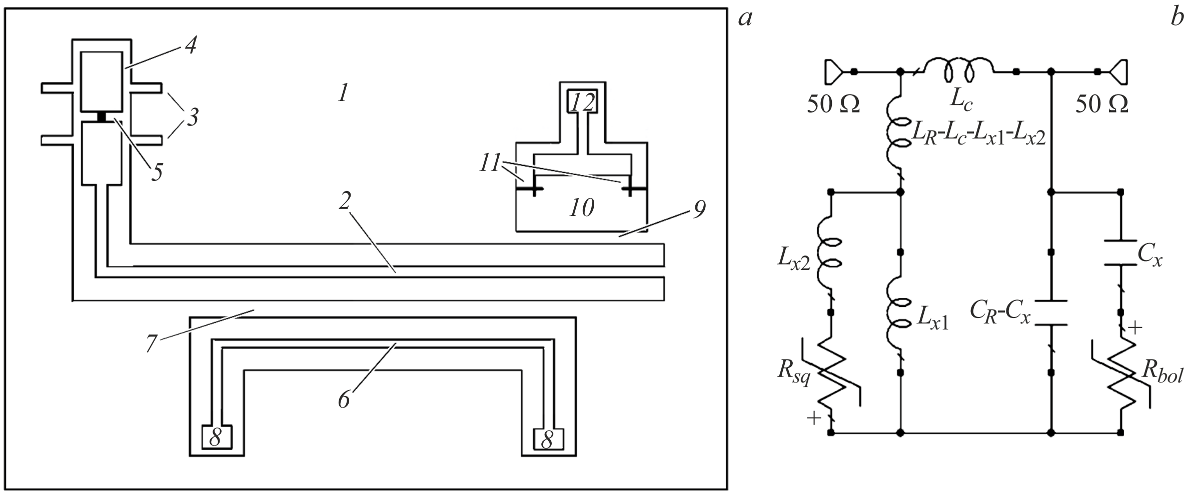

Figure 1. Simplified topology of the active detector (*a*) and its equivalent circuit (*b*): *1* — dielectric substrate coated with a superconducting film; *2* — quarter-wave coplanar resonator; *3* — planar dual-slot antenna with terahertz filters (RFTES detector); *4* — resonator terminal capacitance C_x; *5* — thermoresistive bridge with impedance R_{bol}; *6* — coplanar resonator excitation line; *7* — resonator magnetic coupling element L_c; *8* — ports of the excitation line 50 Ω; elements *9–12* — form a squid amplifier: *9* — squid magnetic coupling element L_{x1}; *10* — squid magnetic loop with inductance L_{x2}; *11* — Josephson junctions; *12* — port of the offset and readout line; R_{sq} — impedance of the ring microwave current in the squid loop.

and the role of a matching impedance transformer between a thermoresistive nanobridge and a squid amplifier.

A high Q-factor ($Q \sim 10^4$) is maintained in a quarter-wave resonator loaded with the active impedance of the bridge R_{bol} and the amplifier R_{sq} by partially including these absorbers in a resonant circuit, the equivalent circuit of which is shown in Fig. 1, *b*. It is shown in the figure that the ohmic losses introduced by R_{bol} and R_{sq} at the resonant frequency can be made arbitrarily small, since the resonator current flowing through each of the absorbers is limited by the magnitude of the capacitive divider C_x/C_R and the inductive divider L_{x1}/L_R. The parameters of the dividers and load resistances are selected so that the equivalent losses from the bridge $R_{bol}(C_x/C_R)^2$ and the squid $Z_0^2(L_x/L_R)^2/R_{sq}$ are equal in operating mode (condition for maximum power transfer).

The search for the equal loss mode (matched mode) in two loads can be carried out using the auxiliary structure of the differential detector [5]. Its circuit is similar to that shown in Fig. 2, *b*, where the second terahertz antenna is connected instead of a squid which is loaded with the same bridge as at the open end of the resonator. Simultaneous heating of the bridge in the antennas leads to the opposite sign of the loss increment in the resonator, therefore, the same heating should not change the Q factor of the resonator. The calculation showed that the inductance of the slot antenna and the squid loop are close, which makes the described balanced structure a convenient measuring platform. Having carried out measurements separately with each detector, we will clarify the calculated switching impedance, which occurs with the same response in the carrier line. We use the electromagnetic modeling method in the AWRD package for clarification, which has confirmed its effectiveness. We can calculate the squid impedance and optimize the matching circuit by conducting the same experiment with a squid: the squid's impedance will match the bridge's impedance if the influence on the resonator is the same like the influence at the bridge. This design allows not only determining the switching impedance of the squid, but, it can be used in the future as a differential detector (null detector).

Figure 2, *a* shows a simplified diagram of the electromagnetic structure of the prototype detector. As a result of the simulation performed to optimize the coupling of the resonator with the excitation line and the geometry of the squid loop for the bridge resistances $\sim 1\,\Omega$, it was possible to effectively transmit a signal to the resistive squid emulator (port 3 in Fig. 2, *a*) located in one of the Josephson contacts *11* (fig. 1, *a*). The efficiency of coupling of the resonator with the communication line is confirmed by a significant variation of the transmission parameter S_{21} in the excitation line when the detector impedance changes. At the same time, the deviation of the bridge impedance from the value of equal losses increasing or decreasing losses in the bridge does not lead to a significant mismatch with the squid.

2. DC-squid modeling

The DC-squid the circuit of which is shown in Fig. 3, *a* was calculated using the RSJ model of two types of resistive shunting of the Josephson junction: tunnel [6] and ohmic. The effect of hysteresis on the current-voltage curve (CVC), which makes it ambiguous can be qualitatively described by taking into account the final capacitance of the

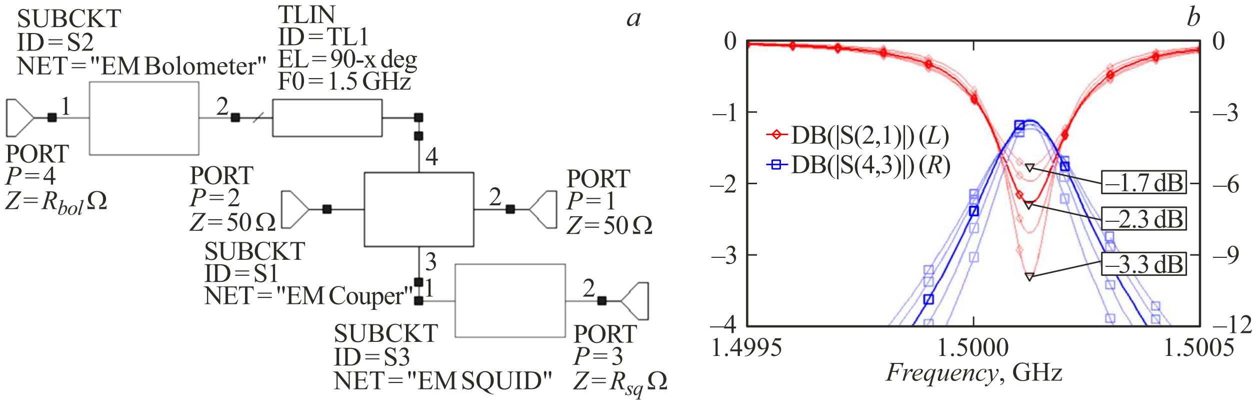

Figure 2. Electromagnetic circuit (model) of the prototype detector (a) and simulation results of scattering parameters (b): S_{21} — signal transmission in the transmission line and S_{43} — matching between the bridge and the squid.

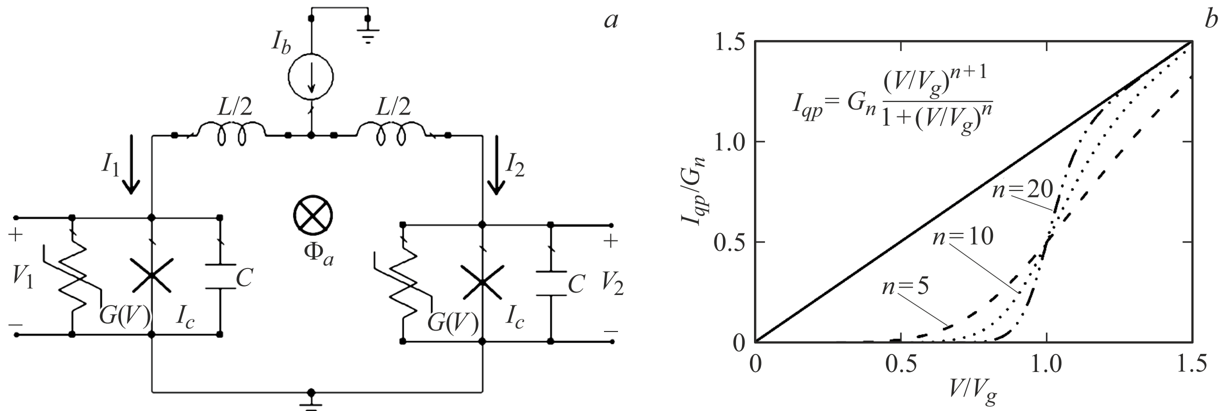

Figure 3. An equivalent squid circuit (a) and an approximation of the VAC tunneling conductivity of the Josephson junction (b) for several values n (a solid line corresponds to a resistor with resistance R_n).

junctions in the resistive-shunted model. The use of a shunt with tunneling conductivity (Fig. 3, b) makes it possible to approximate its impedance by a simple power dependence close to the real dependence of the quasi-particle current in the Josephson junction. The parameter n determines the degree of tunneling conductivity; it was taken equal to 20 in the calculations. The self-induction parameter $\beta_L = 2LI_c/\Phi_0$ determines the degree of parasitic influence of the geometric inductance of the squid loop on the modulation of the critical current by an external magnetic field. $\beta_L \approx 0.4$ is chosen in calculations for junctions with $I_c \sim 5{-}10\,\mu$A and a loop inductance of 50 pH. A hysteresis-free volt-flow characteristic is required when a squid is used as a linear sensor, which means effective damping of Josephson junctions, i.e. the McCumber parameter $\beta_C = 2\pi/\Phi_0 I_c R^2 C$ should satisfy the condition $\beta_C < 1$. The McCumber parameter was set to 0.8 to ensure stable Josephson current over a wide range of offsets.

Fig. 4 shows two squid waveforms corresponding to two types of shunts. It can be seen that there is a significant hysteresis in the CVC ($I_r/I_c \sim 0.8$) for a nonlinear shunt. The installation of resistors with $R_{sh} = R_n$ as shunts turns out to be optimal from the point of view of the amplifying properties of the squid, since it is possible to obtain a stable offset with voltage $V_{bias} \sim V_c$.

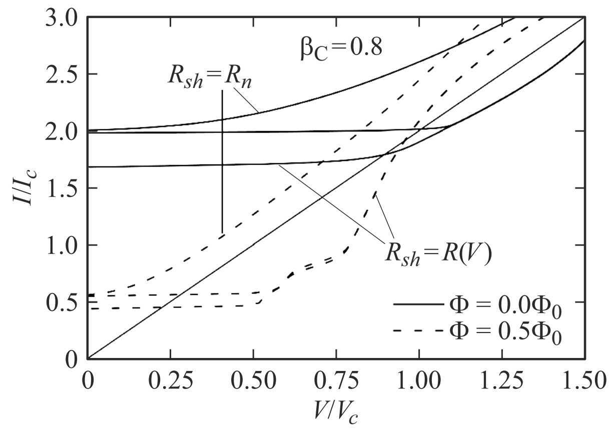

Figure 4. CVC squid under the action of an external magnetic flux for junctions with nonlinear quasi-particle and ohmic conductivity.

A load line 50 Ω is plotted on the CVC in Fig. 5, a, and an operating point with an offset equal to $\approx 0.3V_c$

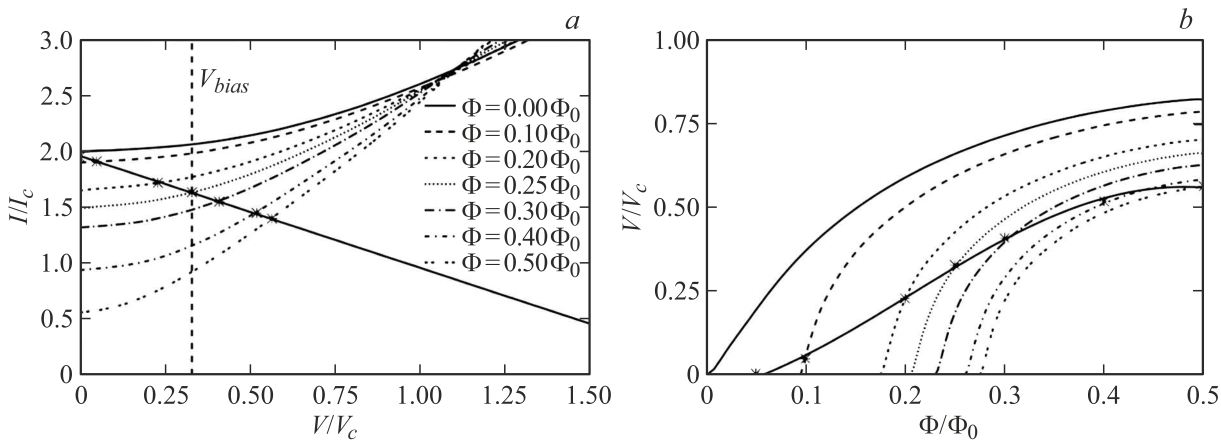

Figure 5. CVC and squid current-flow characteristic for a shunt with a resistor R_n: a — the CVC family and the load line $50\,\Omega$ for a set of values with suppressed critical current; b — volt-flow characteristic of a squid with a load line, as in the figure (a), but rearranged in the coordinate system $V(\Phi)$.

is chosen. The most linear voltage response to a small change of the magnetic flux is achieved at a constant offset $\Phi_a = (2n+1)\Phi_0/4$, when the transmission coefficient $V_\Phi = |\partial V/\partial \Phi_e|$ is maximum. The transmission coefficient at the operating point from Fig. 5, b is equal to $2.7 \cdot 10^{11}$ Hz. The voltage gain $G_V = \partial V_0/\delta V_i$ can be estimated as 20 dB with these parameters.

Let's estimate the saturation level of the squid with the resonator current. The bridge heating current in the operating area is $\sim 1\,\mu$A for the RFTES detector, which is transformed into $\sim 17\,\mu$A at the shorted end of the resonator. The current flowing through the port of the resistive squid emulator does not exceed $1\,\mu$A according to electromagnetic calculation, which is noticeably less than the assumption made above about the critical current of the Josephson junctions that compose the squid. Thus, shunting junctions with $\beta_C < 1$ by relatively high-resistance resistor R_n allows operation at high frequencies of the parametric effect of the Josephson current ≈ 50 GHz, which, according to the idea of the decay of the quantum of Josephson pumping into signal quanta, corresponds to the gain of $G_P \approx f_J/f_s = 15$ dB at a frequency of 1.5 GHz. Effective transmission of the amplified signal from the squid output to the load $50\,\Omega$ can be obtained if the output impedance of the squid Z_{out} at the operating point of the CVC is in the range from 25 to $100\,\Omega$. The dynamic resistance at the squid output will be $R_d \approx 2R_n$ for CVC shown in Fig. 5, so the normal transition resistance is $R_n \approx Z_{out}$.

3. Optimal system transition parameters

The standard approach for obtaining hysteresis-free CVC involves low-ohmic bypass shunting $R_{sh} \ll R_n$, as shown above. The cost of hysteresis suppression is a narrowing of the operating voltage range (Josephson generation) by about an order of magnitude. This limitation can be circumvented by using the junction's own conductivity (self-shunting mode) as a bypass channel, which, as shown above, is not always feasible, and requires high transparency of the tunnel barrier (several atomic layers), however, the probability of multiparticle Andreevsky reflection sharply increases for the case of a thin barrier [7], which leads to a strong uneven dependence of the dynamic resistance on the bias voltage at the junction and reduces the dynamic range of the squid amplifier. The resistivity of the barrier R_nA, equal to the product of the normal transition resistance to its area is the main parameter for evaluating the transparency of the barrier. The parameter β_C can be written as the ratio of the characteristic frequencies ω_c/ω_{RC}. Then the minimum permissible transparency of the barrier ($\beta_C < 1$) is $R_nA < 12\,\Omega \cdot \mu\text{m}^2$ for aluminum junctions with a slit voltage $V_g = 440\,\mu$V and a specific capacitance $C_0 = C/A$ equal to $80\,\text{fF}/\mu\text{m}^2$. Thus, the estimation of the range of normal resistance and transparency of the barrier leads to the need to use submicron junctions with a high critical current density $\sim 30\,\mu\text{A}/\mu\text{m}^2$. The Josephson junction technology based on sandwich structures made of aluminum $Al/AlO_x/Al$, which has been widely applied for the manufacture of qubit circuits, makes it possible to obtain high-quality junctions in a wide range of oxide barrier thicknesses. The development of oxidation modes with low oxygen pressure $\sim 10^{-3}$ mbar and usage of electron lithography will allow obtaining transitions with the parameter $\beta_C < 1$. However, as already noted, the high nonlinearity of the quasi-particle conductivity of tunnel junctions of the SIS type limits the possibility of obtaining a smooth CVC.

It seems possible to suppress the impact of the external system on the squid and obtain a hysteresis-free mode of operation in the absence of low-resistance junction shunting by using damping circuits [2,3], for example, a resistive transmission line for shifting and reading the squid, which can potentially serve as a high-resistance shunt to ensure stable Josephson generation and effective damping of the reactive impedance of external circuits. This factor will be studied in the near future.

Conclusion

The first stage of the development of an active superconducting detector has shown the fundamental possibility of transmitting a signal from a nano-absorber to a squid amplifier while maintaining a consistent mode. The calculation and evaluation of the parameters of Josephson junctions demonstrates certain difficulties in obtaining a squid in the self-shunting mode and leads to the conclusion that it is advisable to use a shunt with a resistance of the order R_n. The estimates performed make it possible to determine a narrow range of process parameters necessary for the manufacture of submicron junctions with a normal resistance close to 50 Ω.

The technology of an active superconducting detector that we develop will allow solving two important tasks in the future:

1) resolution of the problem of broadband matching for a parametric amplifier in the case of a large matrix;

2) obtaining record-low RFTES detector noise by placing gain circuits on the same chip as the detector itself or a matrix of such detectors.

Funding

The study was supported by grant K2-2022-029 within the framework of the Strategic Project „Quantum Internet“ Strategic Academic Leadership Program „Priority-2030“, RNF 24-29-20298 Active Terahertz RFTES detector.

Conflict of interest

The authors declare that they have no conflict of interest.

References

[1] A.V. Merenkov, T.M. Kim, V.I. Chichkov, S.V. Kalinkin, S.V. Shitov. FTT, **64** (10), 1404 (2022) (in Russian). DOI: 10.21883/FTT.2022.10.53081.50HH

[2] G.V. Prokopenko, S.V. Shitov, I.L. Lapitskaya, V.P. Koshelets. J. Mygind. IEEE Trans. Appl. Super Cond., **13** (2), 1042 (2003). DOI: 10.1109/TASC.2003.814146

[3] M. Mueck, R. McDermontt. Supercond. Sci. Technol., **23**, 093001 (2010). DOI: 10.1088/0953-2048/23/9/093001

[4] C.V. Shitov. ZhTF, **93** (7), 988 (2023) (in Russian). DOI: 10.21883/JTF.2023.07.55758.116-23

[5] S.V. Shitov. *Differencial'nyj sverhprovodyashchiy detektor* (Patent RU 2 801 920 C1 RF, IPC H01L 23/00 (2006.01). № 2022134754: appl. 28.12.2022: publ. 18.08.2023)

[6] K. Matsuo. Suppl. Prog. Theor. Phys., **69**, 301 (1980). DOI: 10.1143/PTP.69.301/1894665

[7] V. Patel, J.E. Lukens. IEEE Trans. Appl. Supercond., **9** (2), 3247 (1999).

Translated by A.Akhtyamov